Supplementary information for
Doped Semiconductor-Nanocrystal Emitters with Optimal Photoluminescence Decay Dynamics in Microsecond-Millisecond Range: Synthesis and Applications

Chaodan Pu[a], Junliang Ma[a], Haiyan Qin[a]*, Ming Yan[b], Tao Fu[c], Yuan Niu[a], Xiaoli Yang[a], Yifan Huang[d], Fei Zhao[c], and Xiaogang Peng[a]*

[a]*Center for Chemistry of Novel & High-Performance Materials, and Department of Chemistry, Zhejiang University, Hangzhou, 310027, P. R. China*

[b]*College of Life Information Science and Instrument Engineering, Hangzhou Dianzi University, Hangzhou 310018, China*

[c]*Najing Technology Corporation, 500 Qiuyi Road, Hangzhou 310052, China*

[d]*Department of Chemical and Biological Engineering, Zhejiang University, Hangzhou 310007, China*

Corresponding authors:
Dr. Haiyan Qin (hattieqin@zju.edu.cn)
Prof. Xiaogang Peng (xpeng@zju.edu.cn)

Supplementary information
Method sections

Chemicals

Manganese chloride ($MnCl_2$, 99.999%), stearic acid (HSt), tetramethylammonium hydroxide (25% w/w in methanol), zinc stearate ($ZnSt_2$, ZnO 12.5%~14%), selenium powder (Se, 100 mesh, 99.999%), Zinc Carbonate Hydroxide (97%), cadmium acetate dihydrate (98.5%), 1-octadence (ODE, 90%), oleic acid (HOl, 90%), octylamine, 3-Mercaptopropionic acid (MPA, 97%) were purchased from Alfa-Aesar. Oleylamine (NH_2Ol, 70%), sulfur powder (S, 99.998%) were purchased from Sigma-Aldrich. Sodium diethyldithiocarbamate trihydrate ($NaDDTC{\cdot}3H_2O$, 99%) was purchased from Aladdin Reagents. All organic solvents were purchased from Sinopharm Reagents. Dulbecco's Modified Eagle's Medium (high glucose, DMEM-HG), fetal bovine serum (FBS) and SYTO64 were purchased from GIBCO/Invitrogen (Carlsbad, CA). All other reagents for use in tissue culture were purchased from Sigma Chemical Company (St. Louis, MO). All chemicals were used directly without any further purification unless otherwise stated.

For simplicity, we would employ a systematic abbreviation for fatty amine, fatty acid, and fatty acid salts. For fatty amines, it would be abbreviated as NH_2Xy, where Xy is the first two letters of the common name of the corresponding amine with the first letter of the common name in capital and the second in low case. For example, Oleylamine would be abbreviated as NH_2Ol. For fatty acid and metal fatty acid salts, the abbreviation would be similar to that of fatty amine, but the "NH_2" in the abbreviation would be replaced by either "H" or "M", respectively. For instance, stearic acid and zinc stearate would be written as HSt and $Zn(St)_2$, respectively.

Synthesis

Synthesis of Manganese Stearate ($MnSt_2$): $MnCl_2$ (10 mmol) was dissolved in methanol (20 mL) in a 50 mL flask. In a separate 500 mL flask, HSt (20 mmol) and tetramethylammonium hydroxide (20 mmol) were dissolved in methanol (100 mL) by stirring for 20 min. To this solution, the $MnCl_2$ solution was added dropwise with vigorous stirring. Appearance of white precipitation indicated the formation of $MnSt_2$. After addition of the $MnCl_2$ solution, stirring was continued for 20 min. The white precipitate was washed three times with methanol, and dried under vacuum overnight before using.

$CdSt_2$ was synthesized in a similar method except replace $MnCl_2$ with $CdAc_2$.

Synthesis of cadmium diethyldithiocarbamate trihydrate ($Cd(DDTC)_2$): NaDDTC (20 mmol) was dissolved in distilled water (60 mL). In a separate flask, $CdAc_2{\cdot}2H_2O$ (10

mmol) was dissolved in distilled water (40 mL). To this solution, the NaDDTC solution was added dropwise with vigorous stirring; white precipitation indicated the formation $Cd(DDTC)_2$. After addition of the NaDDTC solution, stirring was continued for 20 min. The precipitate was washed three times with distilled water, and dried under vacuum overnight before using.

Preparation of zinc oleate ($ZnOl_2$) stocks: Zinc carbonate hydroxide and HOl with molar ration 1:4 were loaded into a 50 mL three-neck flask, and ODE was added to adjust the concentration of $ZnOl_2$ to 0.25 M. The mixture was first degassed with argon for 20min before heated to 160 ^oC. After Zinc carbonate hydroxide was completely dissolved by HOl, the solution was allowed to cool down to room temperature for further using.

Synthesis of Mn:ZnSe d-dots: For a typical synthesis, $ZnSt_2$ and $MnSt_2$ with total mole of 0.1 mmol and 5 mL ODE were mixed in a 50 mL three-neck flask. The mixture was degassed at 100 ^oC for 20 min before being heated. Selenium precursor (0.5mmol selenium powder dispersed in 0.6 mL NH_2Ol and 1.4 mL ODE) was swiftly injected into the solution above at 300 ^oC. After reacting for 5 min, the reaction was stopped by cooling down the solution to 200 ^oC. 0.4 mL $ZnOl_2$ stocks was injected, then the temperature was increased to 260 ^oC for ZnSe shell growth. After 10 min, another two 0.4 mL $ZnOl_2$ stocks were subsequently introduced at 10 min interval. Finally, the reaction was stopped by cooling down to room temperature.

For the d-dots with different amounts of Mn^{2+} ions per dot, the amount of $MnSt_2$ was varied by fixing the total amount of the cationic precursors (0.1 mmol) in the initial mixture in the first step described above. Specifically, for the d-dot samples with 32, 71, 96, 187, 241, 338, and 431 Mn^{2+} ions per dot, the amount of $MnSt_2$ was respectively 0.0015, 0.0040, 0.008, 0.016, 0.024, 0.032, and 0.04 mmol.

For purification, Mn:ZnSe d-dots were precipitated with acetone from the original reaction mixture, and then redispersed in hexane. For EDX measurements, in order to obtain the Mn:ZnSe d-dots with high purity, the precipitation was repeated for three times. After purification, the obtained d-dots were dispersed stably in hexane as an optically clear solution.

ZnS shell growth: 4 mL ODE, 1 mL HOl, 1 mL NH_2Ol and as-prepared Mn:ZnSe d-dots in hexane were all loaded into a 50 mL three-neck flask, and heated to 80 ^oC to evaporate hexane. A calculated amount of S stocks (0.75 mmol S powder dispersed in 5 mL ODE) for first ZnS monolayer shell was injected and the reaction solution was headed to 260 ^oC. Then $ZnOl_2$ stocks and S stocks were introduced successively. Each injection was allowed to react for 10 min. When desired thickness was achieved, 1 mL additional $ZnOl_2$ stocks was injected and the reaction was further annealed for 10 min. Mn:ZnSe/ZnS

d-dots were precipitated using hexane and acetone for two times and re-dispersed in hexane for further using.

Synthesis of CdSe/CdS core/shell nanocrystals: The CdSe/CdS core/shell nanocrystals with phase-pure zinc-blende structure were synthesized according to literature[1] with some modifications. Briefly, the zinc-blende CdSe cores (3.1 nm) were synthesized and purified according to our recent reports.[2] For the shell coating, dodecane (3.8 mL), octylamine (1.05 mL), oleylamine (0.45 mL), and purified CdSe core solution (2×10^{-7} mol of nanocrystals) were mixed and heated to 80 °C under an argon flow. Reaction cycles, i.e. addition of the $Cd(DDTC)_2$-amine precursor solutions at 80 °C and growth of CdS monolayers at 150 °C for ~20 min, were applied for the growth of each monolayer. Desirable amounts of $Cd(DDTC)_2$-amine solutions, i.e. 0.08, 0.12, 0.16, 0.21 and 0.26 were used for the growth of first, second, third, fourth, and fifth monolayer, respectively.

Characterization

UV-vis absorption and photoluminescence spectra were measured on an Agilent Cary 4000 UV-vis spectrophotometer and an Edinburgh Instruments FLS920 fluorescence spectrometer. Samples were prepared by dispersing needle-tip aliquots during reaction in hexane. The PL decay dynamics of d-dots were measured by multi-channel scaling (MCS) module of an Edinburgh Instruments FLS920 system. The samples were excited with a μF920H Xe flash lamp at a wavelength of 405 nm and a repetition rate of 50 Hz. For the measurement of PL decay dynamics of CdSe/CdS nanocrystals, the time-correlated single-photon counting (TCSPC) module of the same system was used. A 405 nm picosecond laser diode with a 2 MHz repetition rate was used as the excitation light source.

Transmission electron microscopy (TEM) images were collected on a Hitachi 7700 microscope. Specimens were prepared by putting a drop of hexane solution containing quantum dots on a copper grid coated with thin carbon film.

X-ray powder diffraction (XRD) patterns were obtained using a Rigaku Ultimate-IV X-ray diffractometer operating at 40 kV/40 mA using Cu Kαradiation (λ = 1.5418 Å). Quantum dots for XRD measurement were first precipitated from reaction solution by acetone, and then transferred onto a glass slide for measurement.

Energy dispersive x-ray spectrometry (EDX) was measured on a Hitachi SU-70 microscope. Well-purified D-dots for EDX measurement were transferred onto a piece of glass substrate coated with conductive tape for measurements. Measurements Errors of EDX were found to be about ~2%.

Absolute photoluminescence quantum yield (PL QY) was measured using an Ocean Optics FOIS-1 integrating sphere coupled with a QE65000 spectrometer. d-dots was dispersed in 200 μL hexane with absorbance about 0.1 at 396 nm. A LED lamp with emission peak at 396 nm was used as the excitation source.

Photostability of Mn:ZnSe and Mn:ZnSe/ZnS d-dots was also measured using instrument as that of absolute PL QY measurement.

PL lifetime consistency measurements

PL lifetime of quantum dots in film. Quantum dots films were made by spin-casting the hexane solution of quantum dots onto a glass coverslip. The films were directly used for PL spectra and lifetime measurements.

PL lifetime of quantum dots in aqueous solutions. In order to make quantum dots soluble in water, quantum dots were transferred into water by ligand exchange. In a typical phase transfer procedure, quantum dots in hexane was first precipitated using acetone and dissolved in a small amount of chloroform to form high concentration solution. 50 μL MPA and 300 μL tetramethylammonium hydroxide in methanol and 1 mL methanol were mixed. Appropriate amount of quantum dots in chloroform was injected into the methanol solution for ligand exchange. To ensure complete ligand exchange, this mixed methanol solution was stirred for 30 min at 40 ^{o}C. Subsequently, quantum dots were precipitated using acetic ether twice and re-dispersed in PBS of different pH. The pH values of the aqueous solutions were tuned by adding different amounts of potassium dihydrogen phosphate and sodium hydroxide. This aqueous solutions were used for lifetime measurements.

Temperature dependent PL lifetime of quantum dot solutions was measured using the same system as above with a Julabo F12 heating circulator.

Excitation power dependent PL lifetime measurement was carried out on a time-gated PL lifetime imaging system, which consisted of an Olympus IX83 microscope equipped with an Andor iStar 334T intensified charge-coupled device (ICCD) camera. An Opolette 355 nm pulsed laser with repetition rate of 2 Hz was used as excitation light source and the PL signals were collected by a 20x/0.3 air objective. The excitation and emission lights were filtered and reflected by a filter set containing a dichroic beamsplitter FF458-Di02 and a long pass filter FF01-496 from Semrock. After each excitation pulse illuminated and a delay, a wide field PL image was recorded with a 20 μs gate width. The delay between the first excitation pulse and the opening of the gate was 100 ns, in order to eliminate the autofluorescence from stray lights. As the excitation pulse appeared periodically, the delay time increased linearly by a step of 20 μs. From the time delayed image sequence, the PL decay curve of each individual pixel or the whole field could be

reconstructed. In this measurement, quantum dots solution samples were loaded into a quartz cuvette which was placed horizontally on the specimen stage, the thickness of the solution film was about 300 μm.

Biological autofluorescence-eliminated fluorometry.

Droplets of two d-dots samples with different PL decay lifetime values and different steady-stated PL peaks were added to a bovine serum albumin (BSA) solution (0.1 g BSA in 1 mL water). For the PL lifetime mapping of d-dots and BSA solution sample, the emission wavelength scanning step was set to 5 nm and the measurement time was 45 s for each emission wavelength.

PL lifetime imaging of living cells with d-dots

Cell culture and treatments. RAW264.7 mouse macrophage cells were obtained from the American Type Culture Collection and maintained in DMEM-HG culture medium supplemented with penicillin (100 U/ml), 100 μg/ml streptomycin and 10% fetal calf serum at 37 °C with 5% CO_2. Cells were seeded to 24-well plates (Corning, Tewksbury, USA) at a density of 5×10^4 cells per well. Two solution samples of d-dots with different PL lifetime (200, 550 and 840 μs) were sterilized by membrane filtration (0.22 μm), and then respectively added to confluent RAW264.7 cells at the same concentration. The cells were incubated with the d-dots for 24 h for fluorescence imaging of the engulfed d-dots. After labeling, the cells were washed three times with PBS and detached from the culture plates by gently pipetting. Subsequently, two populations of cells were mixed at equal volumes and cultured together for further imaging.

Lifetime imaging of the mixed cells was carried out on the time-gated PL lifetime imaging system described above. The corresponding bright-field images of the cell samples were collected by an Andor iXon DU-897 electron multiplying charge-coupled device (EMCCD) camera.

PL lifetime multiplexing using commercial high-speed camera

Transfer printing technique was introduced to fabricate a pattern of d-dots for PL lifetime multiplexing. Three d-dot samples with different PL lifetime (86, 220 and 960 μs) were dispersed in ODE solution respectively. SiO_2 powder with diameter about 50~200 nm were added in the solutions to adjust the viscosity of the d-dot inks. Engraved patterns of a circle and characters of “M” and “n” on a steel plate were filled with three d-dots inks respectively. The patterns with d-dots were then transferred to a piece of paper using a rubber by pressing.

The conventional PL image of the pattern illuminated by a UV lamp of 365 nm was recorded by a Canon 70D camera (shutter speed 6.0 s, aperture f/3.5). In order to decode the pattern, time-resolved imaging using a high-speed digital camera was performed. A

CryLas GmbH 355 nm pulsed laser was expanded and illuminated on the pattern with an incident angle of 45°. The maximum energy per pulse was ~30 μJ and the average number of photon absorbed per d-dot per pulse ($\langle N \rangle$) was about 14 calculated from the absorption cross-section of the ZnSe/ZnS core/shell nanocrystals. The pulse duration was 1.4 ns and the repetition rate was 1 kHz. An Olympus i-SPEED high-speed video camera equipped with a Tokina 100 mm f/2.8 AT-X M100 AF PRO lens was placed in front of the pattern to image and record the PL images. A time-resolved PL image sequence was recorded by continuous shooting in a high frame rate of 15 kHz.

The PL intensity decay curve for each individual point on the pattern could be reconstructed by plotting the gray values of the corresponding pixel of all frames. The PL lifetime was obtained by fitting the curve by a single-exponential decay function. At last, with the PL decay lifetime values for all pixels, a spatial resolved PL lifetime mapping was reconstructed.

Alternatively, a more convenient and simple way to decode the pattern is image subtraction. As the PL signal of the three d-dots decayed successively, the pattern composed of d-dots with the longest PL lifetime emerged at the frames in the last section of the sequence (e.g. Frame 8-15). The pattern composed with medium PL lifetime could be decoded by intensity normalizing and then subtracting the long lifetime pattern from the frame in the middle section of the sequence (e.g. Frame 4-7). Similarly, the background pattern with shortest PL lifetime could also be decoded by subtracting the patterns of medium and longest lifetime from the first frame. A decoding imaging in whole was obtained by merging the three patterns of different lifetime together.

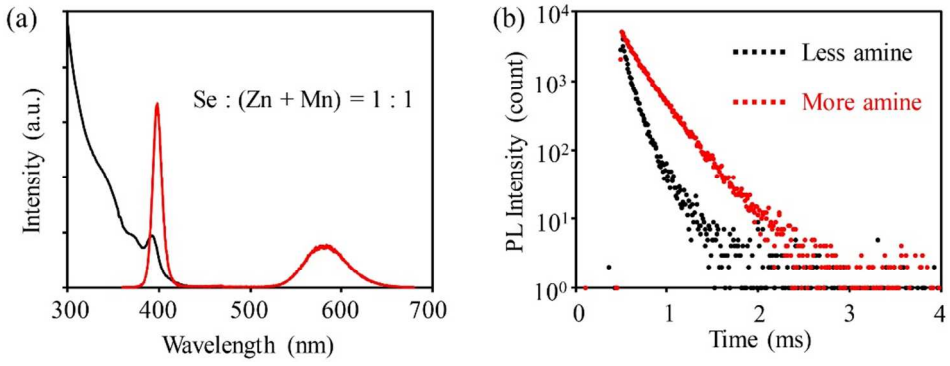

Figure S1. Left: Absorption (black) and PL (red) spectra of Mn:ZnSe d-dots synthesized with 1 : 1 molar ratio of cationic (zinc stearate and manganese stearate) and anionic (selenium) precursors. The intense band-edge PL at around 400 nm indicated nucleation of undoped ZnSe nanocrystals. Right: PL decay curves of Mn:ZnSe d-dots synthesized with 0.6 mL (red) and 0.2 mL (black) oleylamine in 6 ml reaction solutions. In addition to

the original channel represented by the red curve, a short-lifetime channel is evident for the black curve.

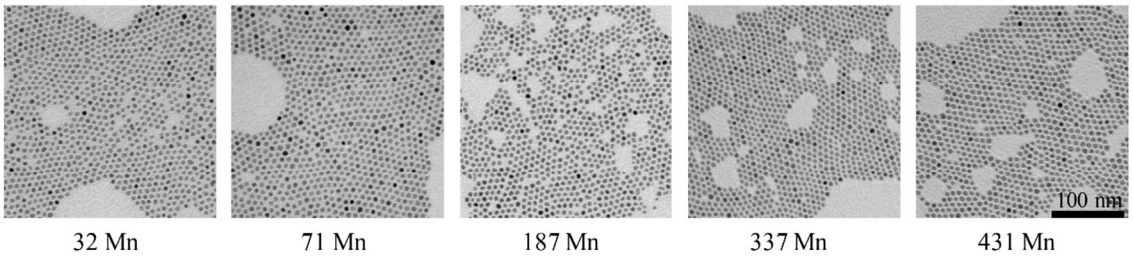

Figure S2. TEM images of Mn:ZnSe d-dots with different amount of manganese ions as labeled under each image. The synthetic procedure for all these samples is provided in the Methods section above.

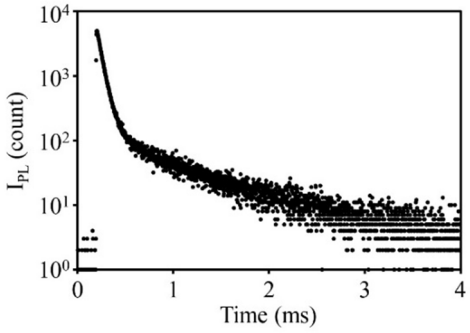

Figure S3. PL decay curves of Mn:ZnSe d-dots synthesized with the nucleation-doping approach. [3] The curve could not be fitted with single-exponential decay and it would be readily to identify one extremely fast component (59 μs) and a slow one (687 μs). The slow one should be associated with Mn ions diffused into the ZnSe host from the original MnSe cluster that was the core for the final d-dots in this well-established approach. The rapid component should be resulted from the remaining part of the MnSe cluster in a d-dot.

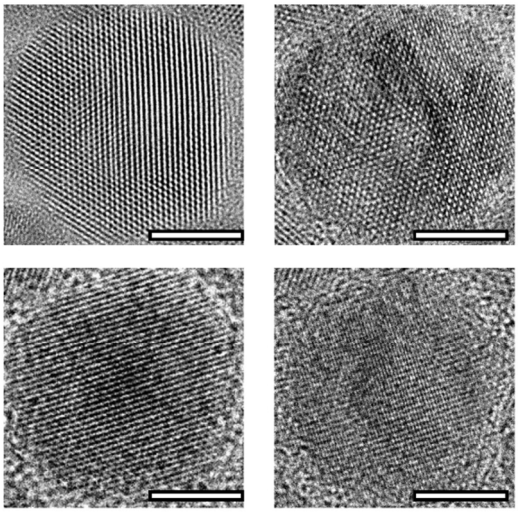

Figure S4. HRTEM images of Mn:ZnSe/ZnS d-dots with different lattice fringes. The scale bar for all four images was 5 nm.

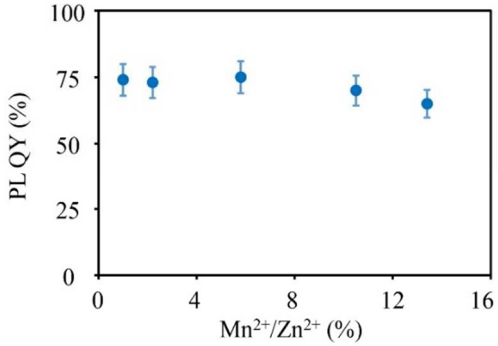

Figure S5. PL QY of Mn:ZnSe/ZnS d-dots with different number of Mn^{2+} ion per dot.

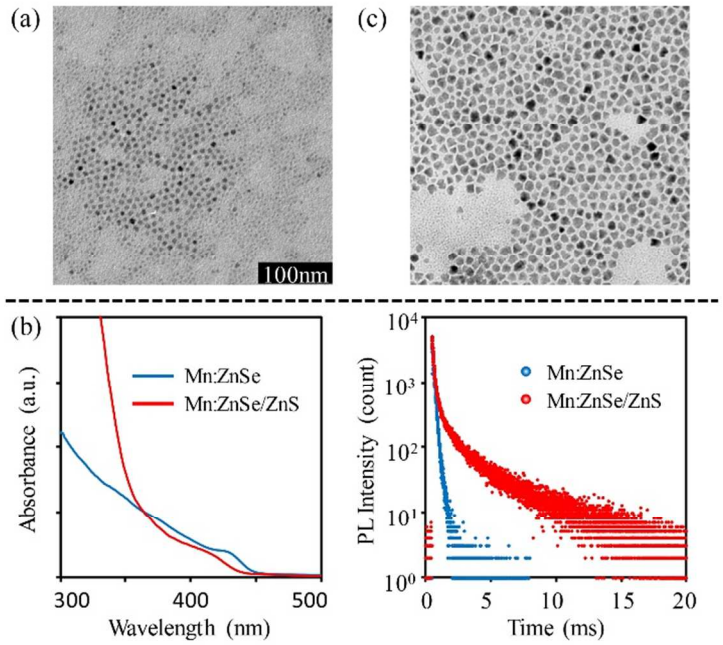

Figure S6. (a) Representative TEM images of the d-dots after the ZnS coating reaction with 1:1 molar ratio of zinc stearate and sulfur. A large amount of tiny ZnS nanocrystals were observed, instead of epitaxial growth onto the Mn:ZnSe d-dots. (b) Significant blue shift of absorption spectra (left) and appearance of long lifetime component (right) upon alloying under conditions of 1:3 ratio of zinc stearate and sulfur. (c) Representative TEM images of Mn:ZnSe/ZnS d-dots synthesized without a sufficient amount of free fatty acids. Although epitaxially growth of ZnS occurred, the size distribution of the resulting nanocrystals was poor.

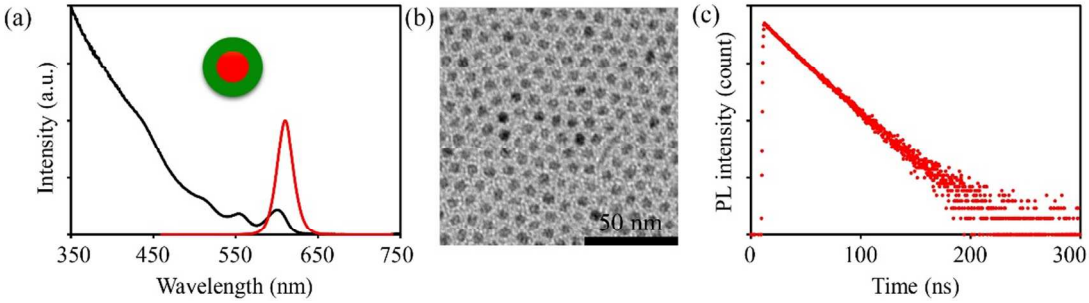

Figure S7. Absorption and photoluminescence spectra (a), TEM images (b), and photoluminescence decay curve (c) of CdSe/CdS core/shell nanocrystals with 5 monolayers of CdS shell in hexane.

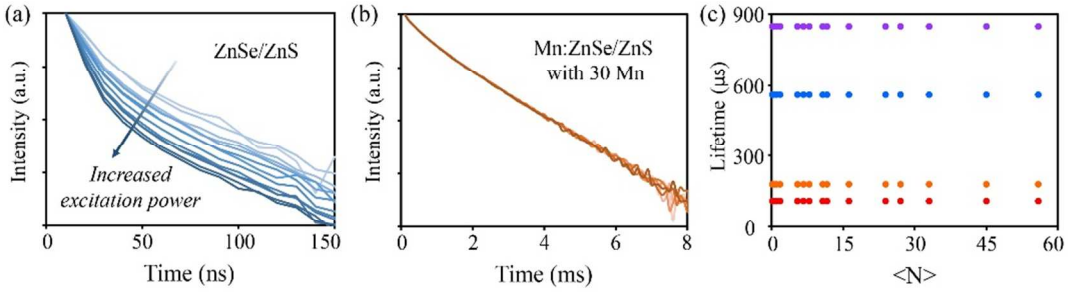

Figure S8. Evolution of PL decay curves of (a) undoped ZnSe/ZnS core/shell nanocrystals and (b) Mn:ZnSe/ZnS d-dots with 30 Mn^{2+} ions upon increasing laser excitation power. ZnSe/ZnS core/shell nanocrystals and Mn:ZnSe/ZnS d-dots used here had the same size of core and shell, and the range of excitation power values were the same for both. In stark contrast to the case of the d-dots, appearance of short lifetime component(s) in the PL decay dynamics was evident upon power increase for the undoped ZnSe/ZnS core/shell nanocrystals. The y-axis for both plots is in logarithm. (c) Statistic results of average photoluminescence decay lifetime of Mn:ZnSe/ZnS d-dots with different single-channel lifetime excited under different excitation power. X axis is the average photon absorbed by one d-dot in one excitation pulse, indicating the average lifetime for all four samples shown in (c) was not influenced by excitation power.

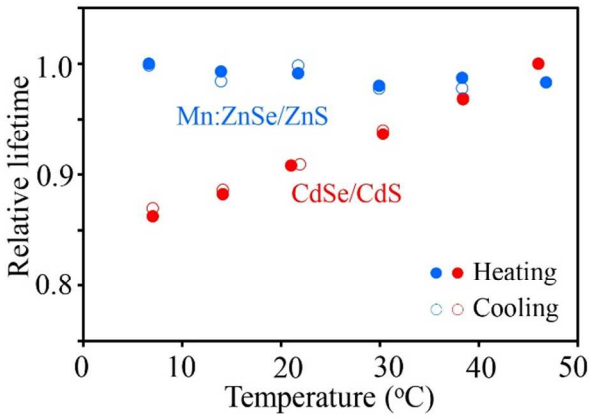

Figure S9. Relative lifetime of Mn:ZnSe/ZnS d-dots (blue) and CdSe/CdS core/shell nanocrystals (red) at different temperatures. The data were recorded for one thermal cycle, and the overlap of relative lifetime indicated the change (or constant) in lifetime was reversible for both samples. Solid spheres represented the data during the heating process and hollow spheres represented the data from the cooling process. For d-dots, almost no change was observed at this temperature range while the deviation was ~20% for that of CdSe/CdS core/shell nanocrystals.

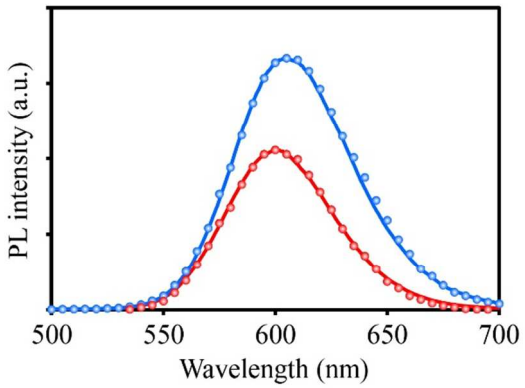

Figure S10. Reconstructed (solid dots) and pure (solid line) photoluminescence spectra of d-dots with 840 μs (red) and 110 μs (blue) lifetime. These results are related to Figure 4 (see related text). The perfect superposition of reconstructed and pure photoluminescence spectra indicated the accuracy of our d-dots in PL lifetime multiplexing.

(1) Qin, H. Y.; Niu, Y.; Meng, R. Y.; Lin, X.; Lai, R. C.; Fang, W.; Peng, X. G. *J. Am. Chem. Soc.* **2014**, *136*, 179-187.

(2) Pu, C. D.; Zhou, J. H.; Lai, R. C.; Niu, Y.; Nan, W. N.; Peng, X. G. *Nano. Res.* **2013**, *6*, 652-670.

(3) Pradhan, N.; Peng, X. G. *J. Am. Chem. Soc.* **2007**, *129*, 3339-3347.